Flow, Turbulence and Combustion
https://doi.org/10.1007/s10494-024-00622-7

BRIEF REPORT

Relation Between 3 and 2D Wrinkling Factors in Turbulent Premixed Flames

Markus Klein[1] · Nilanjan Chakraborty[2]

Received: 29 October 2024 / Accepted: 25 November 2024

Abstract
The magnitude of the wrinkled flame surface area in turbulent premixed flames divided by its projection in the direction of flame propagation, known as the wrinkling factor, is a fundamental quantity for the purpose of analysis and modelling premixed combustion, for example, in flame surface density based modelling approaches. According to Damköhler's hypothesis it is closely related to the turbulent burning velocity, an equally important measure of the overall burning rate of a wrinkled flame. Three-dimensional evaluation of the area of highly wrinkled flames remains difficult and experiments are often based on planar measurements. As a result of this, model development and calibration require an extension of 2D measurements to 3D data. Different relations between 2D and 3D wrinkling factors are known in literature and will be discussed in the present work using a variety of direct numerical simulation (DNS) databases combined with theoretical arguments. It is shown, based on an earlier analysis, that the isotropic distribution of the surface area weighted probability density function of the angle between the normal vectors on the measurement plane and the flame surface, provides a very simple relationship, stating that the ratio between 3D and 2D flame surface area is given by $4/\pi$, which is found to be in excellent agreement with DNS data of statistically planar turbulent premixed flames.

Keywords Flame wrinkling factor · Turbulent premixed flames · Direct numerical simulations

1 Introduction

The flamelet concept allows us to relate the turbulent burning velocity $S_T = \int_V \dot{\omega}_c dV/(\rho_O A_L)$ (where $\dot{\omega}_c$ is the production rate of a suitably defined reaction progress variable c, ρ_0 is the unburned gas density and A_L is the projected area in the direction of flame propagation) to the product of the wrinkled flame area A_T divided by A_L and

✉ Markus Klein
markus.klein@unibw.de

[1] Department of Aerospace Engineering, University of the Bundeswehr Munich, Werner-Heisenberg-Weg 39, 85577 Neubiberg, Germany

[2] School of Engineering, Newcastle University, Claremont Road, Newcastle NE1 7RU, UK

the laminar burning velocity S_L (Smallwood et al. 1995). In fact, Damköhler (Damköhler 1940) suggested the well-known expression,

$$\frac{S_T}{S_L} = \frac{A_T}{A_L} = \Xi^{3D} \Rightarrow S_T = \Xi^{3D} S_L \tag{1}$$

with the quantity Ξ^{3D} known as the wrinkling factor. The validity of this equation has been assessed in several recent works [see Chakraborty et al. (2018) and references therein], showing that it holds only true for statistically planar unity Lewis number flames. Nevertheless, Eq. 1 demonstrates, that the characterization of the wrinkled flame front geometry and morphology is of paramount importance. Similarly, in FSD based modelling the wrinkling factor can be used for expressing the generalized FSD according to Boger (1998) $\Sigma^{3D}_{gen} = \overline{|\nabla c|}$ as

$$\Sigma^{3D} = \Xi^{3D} |\nabla \overline{c}|, \tag{2}$$

where the overbar denotes a Reynolds averaging operation and the subscript has been omitted here and in the following discussion for simplicity. It is important to note that in contrast to Eq. 1 Ξ^{3D} in Eq. 2 can be considered a locally varying quantity. Using the relations $A_T = \int_V \Sigma^{3D} dV$ and $A_L = \int_V |\nabla \overline{c}| dV$, Eq. 1 can be recovered upon volume integration of Eq. 2 and introducing a mean surface averaged wrinkling factor $\left(\Xi^{3D}\right)_S = \int_V \Xi^{3D} |\nabla \overline{c}| dV / \int_V |\nabla \overline{c}| dV$.

Although it has recently been demonstrated (Pareja et al. 2019; Ahmed et al. 2021; Yu et al. 2020; Unterberger et al. 2023; Floyd et al. 2011) that spatial and temporal evolution of the 3D flame structure is possible and provides useful physical insights into the real flame structures, experimental evaluation of 3D isosurfaces is not yet standard. To date, often experimental measurements of flame area, wrinkling and its characterization still depend upon two-dimensional measurements (Shepherd and Ashurst 1992; Kobayashi et al. 1997; Donbar et al. 2000; Shepherd and Cheng 2001; Chen and Bilger 2002; Lachaux et al. 2005; Zhang et al. 2015; Jainski et al. 2017; Chaib et al. 2023). This gives rise to a 2D wrinkling factor Ξ^{2D} which can be expressed as the length of the flame area projected onto a plane to the corresponding lower-dimensional projection, i.e. $\Xi^{2D} = L_T/L_L$. Based on existing DNS databases the present work attempts to assess different relations of the form $\Xi^{3D} = f\left(\Xi^{2D}\right)$.

2 Mathematical Background

Driscoll (2008), in his seminal work, discusses three approaches to estimate 3D surface area from 2D images. (1) The 2D surface density assumption: The DNS data of a slot jet flame by Bell et al. (2007) showed that the value of Σ^{2D} for this particular dataset should be multiplied by 1.35 (Driscoll 2008) to achieve the value of Σ^{3D}. Upon integration of the flame surface density it can be easily seen that for a statistically planar flame, this translates to $A_T/A_L \approx 1.35 L_T/L_L$. (2) The flame perimeter assumption: Here, the value of A_T/A_L is estimated as $A_T/A_L \approx \left(L_T/L_L\right)^2$. This method has been assessed in Driscoll (2008) by considering hypothetical flame wrinkles of rectangular shape or prisms with triangular sides. Based on this hypothetical scenario, the method was reported to have an uncertainty of less than 20%. (3) The fractal dimension assumption: Motivated by the work of Smallwood et al. (1995) A_T/A_L is expressed using fractal theory as $A_T/A_L \approx \left(\epsilon_O/\epsilon_i\right)^{D^{3D}-2}$ where ϵ_O and ϵ_i denote the outer and inner cutoff scale and D^{3D} is the fractal dimension which is approximated from 2D measurements as $D^{3D} = D^{2D} + 1$ based on self-similarity between 2D and 3D. It is worth making the following remarks: The surface density assumption in Driscoll (2008) is based on one single dataset and lacks a theoretical framework. Assuming an isotropic distribution of the surface area weighted probability density function (pdf) of the angle between the normal vectors on the measurement plane and the flame surface it can be shown that $\Sigma^{3D} = 4\Sigma^{2D}/\pi$ (Veynante et al. 2010; Chakraborty and Hawkes 2011) resulting in $(A_T/A_L)/\{(L_T/L_L)(4/\pi)\} = 1$ where Σ^{3D} and Σ^{2D} are the actual 3D flame surface density and the flame surface density estimated based on 2D measurements, respectively. This hypothesis will henceforth be denoted as **HFSD**. It is worth noting that the factor $4/\pi$ is close to the correction factor 1.35 used by Bell et al. (2007). The flame perimeter assumption $(A_T/A_L)/\left(L_T/L_L\right)^2 = 1.0$ (denoted **HPER** in the following) seems to lack a theoretical foundation. It was introduced empirically in Filatyev et al. (2005) and was shown to work reasonably for hypothetical flame wrinkles in Driscoll (2008). Finally, fractal theory is based on the assumption (Smallwood et al. 1995) that $A_T/A_L \approx \left(\epsilon_O/\epsilon_i\right)^{D^{3D}-2}$ or equivalently for 2D projections of the flame $L_T/L_L \approx \left(\epsilon_O/\epsilon_i\right)^{D^{2D}-1}$. Mandelbrot (1983) postulated, based on an isotropic assumption, that $D^{3D} = D^{2D} + 1$ and this relation was found to be reasonably accurate in DNS analyses (Chatakonda et al. 2013; Herbert et al. 2024). Assuming that the inner and outer cutoff scales are the same in 2D and 3D, this shows that $A_T/A_L \approx \left(\epsilon_O/\epsilon_i\right)^{D^{3D}-2} = \left(\epsilon_O/\epsilon_i\right)^{D^{2D}+1-2} \approx L_T/L_L$ or $(A_T/A_L)/(L_T/L_L) = 1.0$, henceforth denoted as **HPLM** because it is based on power-law based modelling. While this last conclusion appears to be trivial, it seems that it has not been pointed out so far. A fourth alternative relation in terms of flame surface density can be found in Veynante et al. (2010). (4) $\Sigma^{3D} = \sqrt{\left(1 + \langle m_y m_y \rangle_S^{2D}\right)} \times \Sigma^{2D}$: where, $m_y = n_y - \langle n_y \rangle_S$ is the fluctuating part of the flame normal vector in the transverse direction and $\langle \cdot \rangle_S$ denotes an appropriate flame surface average. The expression comes from an alternative way of approximating the cosine of the angle between the measurement plane and the flame normal based on the fluctuating components of the flame normal evaluated in 2D. Henceforth it will be denoted **HNFL** (hypothesis based on flame normal fluctuations). It is important to note that HNFL is defined locally, and integral values have to be taken for comparable evaluation in the context of this work (i.e., $(A_T/A_L)/(L_T/L_L)/(\int \sqrt{\left(1 + \langle m_y m_y \rangle_S^{2D}\right)} \times \Sigma_{2D}/\int \Sigma_{2D})$.

Main focus of the present work is to compare it with three alternative expressions and to test all of them for statistically planar turbulent premixed flames for different combustion regimes (and therefore for highly wrinkled as well as mildly wrinkled flames, see Table 1), different chemical mechanisms and stoichiometry, and different treatments of turbulence evolution. The above hypothesis (HFSD, HPER, HPLM, HNFL) will be analysed based on DNS in the next section.

3 Numerical Implementation

Three DNS databases of statistically planar turbulent premixed flames under atmospheric pressure in canonical ‘flame in a box’ configuration have been considered for this analysis. The first DNS database considers stoichiometric methane–air premixed flame-turbulence interaction under decaying turbulence for different turbulence intensities where the chemical mechanism is simplified by a single-step Arrhenius-type irreversible chemistry [for

Table 1 The attributes of the DNS databases considered for this analysis

Case	A1	B1	C1	D1	E1
Database 1 (values at the instant of initialization)					
$u\prime/S_L$	1.0	5.0	7.5	9.0	15.0
l/δ_{th}	4.58	4.58	4.58	4.58	4.58
Da	4.58	0.92	0.61	0.51	0.31
Ka	0.47	5.23	9.60	12.62	27.16
τ	4.5	4.5	4.5	4.5	4.5
Domain size $=45.75\delta_{th} \times \left(45.75\delta_{th}\right)^2$, Grid size $=512 \times 512 \times 512$					

Case	A2	B2	C2	D2	E2
Database 2					
$u\prime/S_L$	1.0	3.0	5.0	7.5	10.0
l/δ_{th}	3.0	3.0	3.0	3.0	3.0
Da	3.0	1.0	0.6	0.4	0.3
Ka	0.58	3.0	6.5	11.9	18.3
τ	4.5	4.5	4.5	4.5	4.5
Domain size $=79.5\delta_{th} \times \left(39.8\delta_{th}\right)^2$, Grid size $=800 \times 400 \times 400$					

Case	A3	B3	C3	D3
Database 3 (values at the instant of initialization)				
$u\prime/S_L$	4.0	8.0	4.0	8.0
l/δ_{th}	3.0	3.0	3.0	3.0
Da	0.75	0.375	0.75	0.375
Ka	4.61	13.06	4.61	13.06
τ	3.77	3.77	5.70	5.70
ϕ	0.4	0.4	0.7	0.7
Domain size	$55.99\delta_{th} \times \left(18.66\delta_{th}\right)^2$	$111.98\delta_{th} \times \left(18.66\delta_{th}\right)^2$	$32.37\delta_{th} \times \left(16.18\delta_{th}\right)^2$	$64.74\delta_{th} \times \left(16.18\delta_{th}\right)^2$
Grid size	$768 \times 256 \times 256$	$1536 \times 256 \times 256$	$504 \times 252 \times 252$	$1152 \times 288 \times 288$

more information please refer to Pfitzner and Klein (2021)]. The second DNS database (Herbert et al. 2024; Ahmed et al. 2019) considers unburned gas forcing for different turbulence intensities, which is realized by using a physical space bandwidth forcing capable of maintaining turbulence intensity and length scale in the unburned gas. This database also considers a single-step Arrhenius-type irreversible chemistry representative of a stoichiometric methane–air mixture. The third DNS database considers lean H_2-air premixed flames with equivalence ratios ϕ of 0.4 and 0.7 under decaying turbulence for different initial turbulence intensities. For this database, a skeletal chemical mechanism (Li et al. 2004) involving 9 species and 19 chemical reactions has been considered and the unburned gas temperature is taken to be 300 K. Mixture averaged transport with Soret and Dufour effects are considered for modelling the transport mechanisms for the lean H_2-air flame database. All the simulations have been conducted using a well-known compressible DNS code SENGA + (Jenkins and Cant 1999; Cant 2012). For all DNS databases considered here, the turbulent velocity fluctuations were initialized using a homogeneous isotropic incompressible velocity field in conjunction with a model spectrum. The reacting flow field is initialized by a steady planar unstrained premixed laminar flame solution. The simulation time in

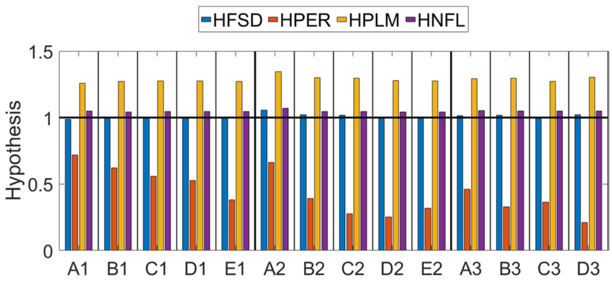

Fig. 1 Diagram of hypothesis HFSD $(\pi/4)(A_T/A_L)/(L_T/L_L)$, HPER $(A_T/A_L)/\left(L_T/L_L\right)^2$, HPLM $(A_T/A_L)/(L_T/L_L)$ and HNFL $(A_T/A_L)/(L_T/L_L)/(\int\sqrt{\left(1+\langle m_y m_y\rangle_S^{2D}\right)}\times\Sigma_{2D}/\int\Sigma_{2D})$, for relating A_T/A_L to L_T/L_L for all cases

all cases remains greater than 2 eddy turnover times and one chemical timescale. Spatial derivatives are approximated using 10th-order central differences. The order of accuracy gradually drops to a one-sided 2nd (for single-step chemistry DNS databases)/4th order (for skeletal chemistry DNS database) scheme at non-periodic boundaries. Time integration is performed using an explicit low-storage Runge–Kutta scheme. Partially non-reflecting in- and outflow (NSBC) boundaries have been specified in the direction of mean flame propagation. The remaining boundaries are considered to be periodic.

The simulation domain size, uniform Cartesian grid used for the discretisation, normalised root-mean-square turbulent velocity fluctuation u'/S_L, normalised integral length l/δ_{th} are listed in Table 1 along with the values of heat release parameter $\tau=(T_{ad}-T_0)/T_0$, Damköhler number $Da=lS_L/u'\delta_{th}$ and Karlovitz number $Ka=\left(u'/S_L\right)^{3/2}\left(l/\delta_{th}\right)^{-1/2}$ where u' is the root-mean-square velocity fluctuation, l is the integral length scale, $\delta_{th}=(T_{ad}-T_0)/\max|\nabla T|_L$ is the thermal flame thickness with T, T_0 and T_{ad} being the dimensional temperature, unburned gas temperature and the adiabatic flame temperature, respectively. The grid spacing for all simulations ensures that the Kolmogorov length scale is resolved and at least 10 grid points are accommodated within δ_{th}.

4 Results

Figure 1 shows the four hypotheses for the relationship between A_T/A_L and L_T/L_L. According to the definition of HFSD, HPER, HPLM and HNFL a value of unity indicates the correctness of the relationship. The values of L_t have been evaluated by determining (and subsequently averaging) the flame length in cut planes aligned with flame mean propagation direction. For cases A3-D3, the reaction progress variable $c=(Y_\alpha-Y_{\alpha u})/(Y_{\alpha b}-Y_{\alpha u})$ is defined based on H_2 mass fraction (i.e., $Y_\alpha=Y_{H_2}$) with subscripts ‘u’ and ‘b’ referring to unburned and fully burned gas values. It can be seen from Fig. 1 that HFSD assumes values very close to unity, whereas HPLM, which assumes a proportionality as well between A_T/A_L and L_T/L_L, has a constant overprediction of about $4/\pi\approx1.273$. By contrast, HPER shows the strongest deviations in a quantitative manner but also the qualitative trend is wrong because the deviations increase considerably with increasing turbulence intensity.

The HFSD, HNFL and HPLM are based on some sort of isotropic assumption, which seems to indicate a proportionality between A_T/A_L and L_T/L_L. In addition, HPLM assumes that the outer and inner cutoff scales are the same for a 2D and 3D evaluation. While there is some indication that 2D and 3D inner cutoff scales might have the same order of magnitude (Herbert et al. 2024), there is a considerable amount of uncertainty remaining, regarding this last assumption. The HPER assumption $A_T/A_L \sim \left(L_T/L_L\right)^2$ is mathematically tempting based on dimensional grounds. However, it is not supported by the present analysis. Driscoll (2008) reported reasonable performance of relation HPER for hypothetical surface wrinkles of rectangular shapes or prisms with triangular sides, provided the aspect ratio is lower than unity. In addition, it was reported in Filatyev et al. (2005) that HPER displays similar trends as a S_T/S_L versus u'/S_L diagram. The fact that HFSD and HPLM perform considerably better than HPER, suggests that turbulent flame surfaces are much more complex than wrinkles of rectangular shape or prisms with triangular sides, and probably are indeed characterised by a fractal-like behaviour at least for a limited range of scales. The relation HNFL shows similar, but slightly worse, performance to that of HFSD. Moreover, the evaluation of surface-averaged flame normal will be challenging for binarised flame images in experiments. Finally, a relation similar to HNFL, which involved the flame normal fluctuation in the direction of flame propagation m_x (Halter et al. 2009), as well as an approximate expression similar to HNFL based on the isotropic distribution of flame normal fluctuations (Veynante et al. 2010), does not work satisfactorily because of the non-isotropic nature of flame normal fluctuations.

The present work is based on DNS data of statistically planar turbulent premixed flames, featuring a resolution that is higher than the one typically achievable in experimental work. However, filtering the flame front with a filter up to a filter width of $\Delta_f/\delta_{th} = 2$ does not change the ratio $(A_T/A_L)/(L_T/L_L)$ by more than 3–4%. It is also worth noting that the HFSD relation does not only work for statistically planar premixed flames interacting with homogeneous isotropic turbulence but was also shown to be valid for turbulent premixed Bunsen and jet flames (Hawkes et al. 2011; Wang et al. 2021).

5 Conclusions

Existing, DNS databases of statistically planar turbulent premixed flames have been used to assess different relations between flame wrinkling observed in 3D space and 2D projections. Based on theoretical arguments from the literature, it can be shown that A_T/A_L and L_T/L_L are proportional to each other using isotropy assumptions and the DNS data showed excellent agreement with the theoretical prediction of the constant of proportionality, i.e. $A_T/A_L = (4/\pi)L_T/L_L$. It will be worthwhile to study in future under which circumstances the assumptions of isotropy break down, which might happen in the presence of flame instabilities, for very low turbulence intensities or in a different flame configuration.

Author Contributions Both authors contributed equally to this work.

Funding Open Access funding enabled and organized by Projekt DEAL. This research was funded by Engineering and Physical Sciences Research Council UK (EP/W026686/1, EP/X035484/1) and dtec.bw—Digitalization and Technology Research Center of the Bundeswehr; dtec.bw is funded by the European Union—NextGenerationEU.

Data Availability No datasets were generated or analysed during the current study.

Declarations

Conflict of interest The authors declare no competing interests.

Ethical Approval The authors complied with all ethical standards relevant to this work.

References

Ahmed, U., Chakraborty, N., Klein, M.: Insights into the bending effect in premixed turbulent combustion using the flame surface density transport. Combust. Sci. Technol. **191**, 898–920 (2019)

Ahmed, P., Thorne, B., Lawes, M., Hochgreb, S., Nivarti, G.V., Cant, R.S.: Three dimensional measurements of surface areas and burning velocities of turbulent spherical flames. Combust. Flame **233**, 111586 (2021)

Bell, J.B., Day, M.S., Grcar, J.F., Lijewski, M.J., Driscoll, J.F., Filatyev, S.A.: Numerical simulation of a laboratory-scale turbulent slot flame. Proc. Combust. Inst. **31**, 1299–1307 (2007)

Boger, M., Veynante, D., Boughanem, H., Trouvé, A.: Direct numerical simulation analysis of flame surface density concept for large eddy simulation of turbulent premixed combustion. Proc. Combust. Inst. **27**, 917–925 (1998)

Cant, R.S.: SENGA2 Manual, CUED-THERMO-2012/04, Cambridge University, 2nd edn, Cambridge, UK (2012)

Chaib, O., Zheng, Y., Hochgreb, S., Boxx, I.: Hybrid algorithm for the detection of turbulent flame fronts. Exp. Fluids **64**, 104 (2023)

Chakraborty, N., Hawkes, E.R.: Determination of 3D flame surface density variables from 2D measurements: validation using Direct Numerical Simulation. Phys. Fluids **23**, 065113 (2011)

Chakraborty, N., Alwazzan, D., Klein, M., Cant, R.S.: On the validity of Damköhler's first hypothesis in turbulent Bunsen burner flames: a computational analysis. Proc. Combust. Inst. **37**, 2231 (2018)

Chatakonda, O., Hawkes, E.R., Aspden, A.J., Kerstein, A.R., Kolla, H., Chen, J.H.: On the fractal characteristics of low Damköhler number flames. Combust. Flame **160**, 2422–2433 (2013)

Chen, Y.C., Bilger, R.W.: Experimental investigation of three-dimensional flame-front structure in premixed turbulent combustion—I: hydrocarbon/air bunsen flames. Combust. Flame **131**, 400–435 (2002)

Damköhler, G.: Der Einfluss der Turbulenz auf die Flammengeschwindigkeit in Gasgemischen. Zeitschrift Für Elektrochemie und Angewandte Physikalische Chemie **46**, 601–626 (1940)

Donbar, J.M., Driscoll, J.F., Carter, C.D.: Reaction zone structure in turbulent non-premixed jet flames from CH–OH PLIF images. Combust. Flame **122**, 1–19 (2000)

Driscoll, J.F.: Turbulent premixed combustion: flamelet structure and its effect on turbulent burning velocities. Prog. Energy Combust. Sci. **34**, 91–134 (2008)

Filatyev, S.A., Driscoll, J.F., Campbell, D., Carter, J., Donbar, J.M.: Measured properties of turbulent premixed flames for model assessment, including burning velocities, stretch rates, and surface densities. Combust. Flame **141**, 1–21 (2005)

Floyd, J., Geipel, P., Kempf, A.M.: Computed tomography of chemiluminescence (CTC): instantaneous 3D measurements and Phantom studies of a turbulent opposed jet flame. Combust. Flame **158**, 376–391 (2011)

Halter, F., Chauveau, C., Gokalp, I., Veynante, D.: Analysis of flame surface density measurements in turbulent premixed combustion. Combust. Flame **156**, 657–664 (2009)

Hawkes, E.R., Sankaran, R., Chen, J.H.: Estimates of the three-dimensional flame surface density and every term in its transport equation from two-dimensional measurements. Proc. Combust. Inst. **33**, 1447–1454 (2011)

Herbert, M., Chakraborty, N., Klein, M.: A Comparison of evaluation methodologies of the fractal dimension of premixed turbulent flames in 2D and 3D using direct numerical simulation data. Flow Turbul. Combust. (2024). https://doi.org/10.1007/s10494-024-00560-4

Jainski, C., Rißmann, M., Böhm, B., Dreizler, A.: Experimental investigation of flame surface density and mean reaction rate during flame–wall interaction. Proc. Combust. Inst. **36**, 1827–1834 (2017)

Jenkins, K.W., Cant, R.S.,: DNS of turbulent flame kernels. In: Liu, C., Sakell, L., Beautner T. (eds.) Proceedings of the Second AFOSR Conference on DNS and LES, pp. 192–202, Kluwer Academic Publishers (1999)

Kobayashi, H., Nakashima, T., Tamura, T., Maruta, K., Niioka, T.: Turbulence measurements and observations of turbulent premixed flames at elevated pressures up to 3.0 MPa. Combust. Flame **108**, 104–110 (1997)

Lachaux, T., Halter, F., Chauveau, C., Gokalp, I., Shepherd, I.G.: Flame front analysis of high-pressure turbulent lean premixed methane–air flames. Proc. Combust. Inst. **30**, 819–826 (2005)

Li, J., Zhao, Z., Kazakov, A., Dryer, F.: An updated comprehensive kinetic model of hydrogen combustion. Int. J. Chem. Kinetics **36**, 566–575 (2004)

Mandelbrot, B.B.: The fractal geometry of nature. Freeman, New York (1983)

Pareja, J., Johchi, A., Li, T., Dreizler, A., Böhm, B.: A study of the spatial and temporal evolution of auto-ignition kernels using time-resolved tomographic OH-LIF. Proc. Combust. Inst. **37**, 1321–1328 (2019)

Pfitzner, M., Klein, M.: A near-exact analytic solution of progress variable and pdf for single-step Arrhenius chemistry. Combust. Flame **226**, 380–395 (2021)

Shepherd, I.G., Ashurst, W.T.: Flame front geometry in premixed turbulent flames. Proc. Combust. Inst. **24**, 485–491 (1992)

Shepherd, I.G., Cheng, R.K.: The burning rate of premixed flames in moderate and intense turbulence. Combust. Flame **127**, 2066–2075 (2001)

Smallwood, G.J., Gülder, Ö.L., Snelling, D.R., Deschamps, B.M., Gökalp, I.: Characterization of flame front surfaces in turbulent premixed methane/air combustion. Combust. Flame **101**, 461–470 (1995)

Unterberger, A., Martins, F.J.W.A., Mohri, K.: Coupled 3D evolutionary reconstruction technique for multi-simultaneous measurements. Fuel **346**, 128336 (2023)

Veynante, D., Lodato, G., Domingo, P., Vervisch, L., Hawkes, E.: Estimation of three-dimensional flame surface densities from planar images in turbulent premixed combustion. Exp. Fluids **49**, 267–278 (2010)

Wang, H., Hawkes, E.R., Ren, J., Chen, G., Luo, K., Fan, J.: 2D and 3D measurements of flame stretch and turbulence-flame interactions in turbulent premixed flames using DNS. J. Fluid Mech. **913**, A11 (2021)

Yu, T., Wang, Q., Ruan, C., Chen, F., Cai, W., Lu, X., Klein, M.: A quantitative evaluation method of 3D flame curvature from reconstructed flame structure. Exp. Fluids **61**, 66 (2020)

Zhang, M., Wang, J., Jin, W., Huang, Z., Kobayashi, H., Ma, L.: Estimation of 3D flame surface density and global fuel consumption rate from 2D PLIF images of turbulent premixed flame. Combust. Flame **162**, 2087–2097 (2015)